



Published in final edited form as:

Methods Mol Biol. 2012 ; 884: 53–69. doi:10.1007/978-1-61779-848-1_4.

Subretinal delivery and electroporation in pigmented and nonpigmented adult mouse eyes

John M. Nickerson¹, Penny Goodman¹, Micah A. Chrenek¹, Christiana J. Johnson¹, Lennart Berglin^{1,2}, T. Michael. Redmond³, and Jeffrey H. Boatright¹

¹Department of Ophthalmology, Emory University, Atlanta, GA

²St. Erik's Eye Hospital, Karolinska Institutet, Stockholm, Sweden

³National Eye Institute, National Institutes of Health, Bethesda, MD

Abstract

Subretinal injection offers one of the best ways to deliver many classes of drugs, reagents, cells and treatments to the photoreceptor, Müller, and retinal pigment epithelium (RPE) cells of the retina. Agents delivered to this space are placed within microns of the intended target cell, accumulating to high concentrations because there is no dilution due to transport processes or diffusion. Dilution in the interphotoreceptor space (IPS) is minimal because the IPS volume is only 10-20 microliters in the human eye and less than 1 microliter in the mouse eye.

For gene delivery purposes, we wished to transfect the cells adjacent to the IPS in adult mouse eyes. Others transfect these cells in neonatal rats to study the development of the retina. In both neonates and adults, electroporation is found to be effective. Here we describe the optimization of electroporation conditions for RPE cells in the adult mouse eye with naked plasmids.

However, both techniques, subretinal injection and electroporation, present some technical challenges that require skill on the part of the surgeon to prevent untoward damage to the eye. Here we describe methods that we have used for the past ten years (1).

Keywords

subretinal; injection; electroporation; interphotoreceptor space; transfection; dilation; sclera; cornea; reporter gene expression; subretinal bleb

1. Introduction

The subretinal space is a useful target for drug delivery (2, 3-6) and gene therapy purposes (7-21) because subretinal delivery places injected material within microns of the plasma membranes of the photoreceptor (PhR), Mueller, and the retinal pigment epithelium (RPE) cells. It is important that in many cases, detached retina rejoins the RPE sheet quickly, a process called bleb regression. Once the bleb has regressed the reattached retina functions again. Subretinal injection surgery is used clinically (cf., tPA injection for submacular or subretinal hemorrhage) (22, 23) and has been demonstrated in many animal models (4, 5, 6).

Genetics and genomic modifications in the mouse are facile and highly informative, making the mouse the “go-to” animal in much of biomedical research and in particular in vision

research. It is the smallest mammal that has an eye resembling the human counterpart. However, the small size of the eye and the relatively large size of the lens make subretinal surgery difficult in mice. Several surgical approaches have evolved for the mouse.

Many research groups have reported a transscleral route for subretinal injections. In this route, a needle is advanced through the sclera, entering at the limbus or pars plana, crossing through the vitreous, penetrating through the diametrically opposite retina into the subretinal space. Another route is a transscleral-transchoroidal-Bruch's membrane approach without penetrating the retina (24, 25, 26, 27). Both routes are effective for injecting many materials in fluid form, and in collecting the contents of the interphotoreceptor (subretinal) space. However, the small size of the mouse eye and the comparative toughness of the sclera increase the risk of accidentally induced hemorrhages at the ciliary body or choroid. These hemorrhages cause autofluorescence and retinal damage, rendering further treatment or experimentation futile. To solve the problem of hemorrhages, Timmers and coworkers (28) developed a subretinal injection approach in rats via a transcorneal route. We adapted this route to the mouse as described here.

There are many ways to transfect DNA into a target cell, including viruses (29, 30), physical (electroporation, ballistic, and sonication) (31-35), chemical (liposomes (36, 37), DNA compaction (38), dendrimers (39), and precipitates—e.g., calcium phosphate) (40). Of these, viruses achieve 100% transduction efficiency in cultured photoreceptor cells (17) and electroporation achieves up to 90% transfection efficiency (41). Other chemical-based agents may be highly successful but often require serum-free conditions (42), a state that is impossible in vivo.

Electroporation is inexpensive, safe, and easy to replicate under well-controlled conditions (32, 33, 41). Initially we found electroporation to work erratically in mice, but once we standardized our protocols (28), we found it to work well. Here we detail steps that we found essential for consistent results. A key step was to evaluate the fundus after the subretinal injection. Here, we present videos of the surgical technique so that others can more readily learn subretinal injection, as initially described in rats by Timmers and coworkers (28). Given more reliable surgery, it was possible to optimize electroporation to deliver plasmids to RPE cells. These conditions show high-level reporter gene expression from plasmids in the RPE of the living adult mouse (1).

2. Materials

1. A HOBO datalogger records data every 5 min for a week or a month (Lab Safety Supply; U12-012, \$133.00; HOBO software \$89.00) and is used to measure light level, temperature, and humidity in animal care rooms and elsewhere.
2. Reporter gene plasmid: The reporter expression plasmid, called pVAX-tdTomato (43), contained the CMV Immediate Early promoter driving expression of tdTomato. This plasmid contains a bovine growth hormone poly(A) signal on the 3' flanking side of the tdTomato cDNA. The plasmid contains the Kanamycin resistance gene for selection and growth. This plasmid was a kind gift from Dr. Ton N.M. Schumacher of the Department of Immunology, The Netherlands Cancer Institute, Amsterdam, The Netherlands. Plasmid was isolated from transformed DAM⁻/DCM⁻ cells (catalog number C2925H) from New England Biolabs. *Escherichia coli* are grown overnight in Luria broth using a Qiagen Endotoxin Free GIGAprep kit following the manufacturer's protocol. Plasmid pellet is dissolved using molecular grade water. 50 µg of plasmid is dried using a speedvac system. Pellets are stored in the -20 °C until needed.

3. Dissecting microscope system: We use an Olympus SZX2-ZB16 stereo microscope (Hunt Optics; Pittsburgh, PA), which is equipped with a halogen lamp mounted to an epifluorescence adapter with no fluorescence filters (we have also tried a ring light and a co-axial illuminator). This light source gives true coaxial illumination through the objective lens which is far better than a ring light for illuminating the back of the mouse eye. The new light is about 8 times brighter than the previously described coaxial light source (1). The improved light source is important for the subretinal injection of pigmented mice. It is bright enough to make the injection of pigmented mice easy, fast, and practical.
4. Video recording: These are conducted with a Panasonic GPUS932HT HD Video camera (Hunt Optics and Imaging). The camera was interfaced to a KONA LHe HD-video capture card (AJA Video Systems, Grass Valley, CA) installed in a Mac Pro (Apple Computer, Cupertino, CA) running OSX Snow Leopard 10.6.8. Videos were edited with Final Cut Pro (version 6; Apple Computer). Video recordings are optional, but helpful for training and demonstration purposes.
5. Injection equipment: We use a NanoFil™ Sub-microliter injection system with a UMP-II microsyringe pump and Micro4 controller with a footswitch (World Precision Instruments; WPI, Sarasota, FL).
6. It is important to maintain the mouse at body temperature during and after anesthesia. We use two systems to maintain the mouse at 37 °C. One is an in-house developed aluminum block having channels cut in it for warm water circulation, with the block temperature controlled with a Lauda Circulating water bath. The second system is a commercial product, a T/Pump TP500; Gaymar, Orchard Park, NY.
7. Beveled 34 gauge needles (catalog number NF34BV-2), blunt 35 gauge needles (catalog number NF35BL-2), and curved forceps (catalog number 15915) were obtained from WPI. Most other incidental equipment and tools were from Fisher Scientific (Pittsburgh, PA) or VWR (West Chester, PA).
8. Vidisic^R Augengel (catalog number 1-19006, distributed by Dr. Mann Pharma, Berlin, Germany) is a transparent clear ocular hydro-gel, which contains high molecular weight polyacrylic acid. It was the kind gift of Dr. Philipp Lirk, Department of Anesthesiology and Critical Care Medicine, Medical University Innsbruck, Austria. Other clear ophthalmic grade hydrogels, including viscous methylcelluloses are acceptable as well.
9. Quantum dots with a 600 nm fluorescence emission maximum (EviTags, E2-C11-NF2-0600; Evident Technologies, Troy, NY) were injected as the stock preparation. This source is no longer available, but similar quantum dots and other fluorescent spheres can be obtained from Invitrogen (Carlsbad, CA) to mark the bounds of a subretinal injection.
10. The electroporator was a commercial square wave generator (BTX model ECM830; Harvard Apparatus, Holliston, MA). Others are acceptable, too.
11. Platinum-iridium 20 gauge wire (catalog number 50822164; Fisher).
12. Small test-jumper leads (catalog number 278-001; Radio Shack Corporation, Fort Worth, TX).
13. Apoptotic cells are detected with a DeadEnd TUNEL kit (product number G3250; Promega, Madison, WI) used according to the manufacturer's instructions.

14. Pre-mixed 80mg/ml and 12mg/ml Ketamine and Xylazine solution (K-113; Sigma-Aldrich, St. Louis MO).
15. Phenylephrine, (2.5% W/V; ophthalmic grade; Bausch & Lomb, Tampa, FL)
16. Proparacaine hydrochloride ophthalmic solution USP, 0.5%; National Drug Code (NDC) 17478–263–12; Akorn Inc., Buffalo Grove, IL.
17. Optispears (Ocusoft, Inc., Richmond, TX)
18. “Refresh” eye drops (Allergan, Irvine, CA)
19. Microknife. (Blade size 15° stab knife straight, Sharpoint, catalog number REF72-1501, Reading, PA)

3. Methods

1. Mouse husbandry: Mice should be used according to ARVO guidelines and must be approved by a local Institutional Animal Care and Use Committee. Mice were housed at 22 °C in facilities managed by the Emory University Division of Animal Resources and given standard mouse chow (Lab Diet 5001; PMI Nutrition Inc., LLC, Brentwood, MO) and water ad libitum. They were maintained on a 12 h:12 h light-dark cycle, with daytime lighting ranging 200–750 lux outside the cage depending on lower, middle, or top shelf position of the cage rack. We have found it useful to monitor light levels, temperature, and humidity with a datalogger. This can identify unexpected changes in lighting, humidity, or temperature that can alter the outcomes of any in vivo study (a sample record showing a stuck light switch, a light bulb burning out, and a humidity spike are illustrated in Figure 1).

2. Strains: We have used pigmented and nonpigmented mice aged between birth and 9 months old at time of surgery. We do not think that there would be a need to modify the protocol for older mice, but we have not tested mice older than 10 months. For neonatal mice, the procedure of (24) is fast and easy.

3. Injection material preparation: Resuspend plasmid DNA (pVAX-TdTomato) in sterile water at 2 mg/ml. The marker dye Fast Green (catalog number BP123-10, Fisher, Fairlawn, NJ) is included in all injected solutions at 0.1% (W/V). Centrifuge the plasmid solution at $10,000 \times g$ for 5 min to sediment any particulates from the solution that might clog a 35 gauge needle. Do this immediately before loading the needle and injection syringe (Figure 2).

4. Surgical sterility: Use sterile surgical technique throughout. Sterilize fluid lines, surgical instruments, and needles by repeated rinsing with 70% ethanol and sterile water.

5. Anesthesia: Perform injections between 8:00 AM and 6:00 PM (i.e., during lights-on of the photoperiod). Keep each mouse on a 37 °C pad during and after surgery until it regains consciousness and mobility. Mice are anesthetized with 80 mg ketamine and 12 mg xylazine per kilogram body weight (K-113; Sigma-Aldrich, St. Louis, MO) and achieve adequate anesthesia in 3 to 5 min.

Ketamine/Xylazine preparation: To make a working solution, dilute the stock 1:5 with sterile dPBS. Keep the working solution ice cold at all times. The working concentration is 16 $\mu\text{g}/\mu\text{l}$ Ketamine and 2.4 $\mu\text{g}/\mu\text{l}$ Xylazine. So, for a 20 g mouse, 100 μl are injected into the hind leg muscle with a 29 gauge needle. Be sure to record these drugs accurately in a suitable logbook following DEA regulations.

Anesthetize the cornea topically with one drop of proparacaine for 2 min. Remove excess with an optispear. Add a drop of Refresh artificial tears on the eye to prevent drying, and remove excess.

Add one drop of Phenylephrine, and wait 2-3 min. Place the animal on the heating pad and cover to shield from light to help dilate the pupils. (A cardboard boxtop covering the entire mouse that does not impede airflow is adequate. The pupil should be fully dilated within 90 seconds. If not dilated, apply another drop of phenylephrine.

When moving to the injection scope, remove excess phenylephrine with an Optispear. Place the mouse on the heated stage to maintain body temperature during surgery. Mice should be monitored carefully for signs of pain and distress during and after surgery.

6. Figure 3 provides static images of the subretinal injection technique. Position the mouse with its nose pointing away from the surgeon and its left eye facing up toward the light and the microscope. Place a drop of hydrogel (Vidisc^R) on the mouse cornea. Grasp the corner of a 22×40 microscope coverslip by hand and adjust the coverslip on the Vidisc^R eye gel in such a way that the fundus, its blood vessels, and the optic nerve head can be seen. Verify that the pupil is fully dilated. This fundus exam serves to assess the condition of the eye before injection and as a comparison for the postoperative condition of the retina. Note the structure and appearance of blood vessels and optic disc. (For pigmented animals, the lighting should be about 54,000 lux, and for nonpigmented the light source should be about 4800 lux (adjust with neutral density filters to reduce the light level, or use another source).

Adjust the position the mouse on a heating pad as necessary for the surgical procedure. It is not necessary or desirable to restrain the mouse. Remove excess Vidisc with an Optispear. Apply Betadine (5%, ophthalmic grade, Alcon, NDC 0065 0411 30; Ft. Worth TX) to eye, lids, and fur surrounding eye. Remove excess with an Optispear. At this point, it should take about 90 seconds to complete the subretinal injection. Grasp the left eye with curved forceps held in the surgeon's left hand so that the eye is slightly proptosed by partially and gently closing the forceps. With a 34 gauge beveled needle (held in the surgeon's right hand) lance the cornea near the limbus penetrating into the anterior chamber at an oblique (nearly tangential) angle (Figure 3C). Some stretching of cornea is advantageous, allowing the wound to effectively reseal itself at the end of surgery. Remove the beveled needle. Replace it with a blunt 35 gauge needle connected to the injection system (WPI). Advance the needle into the anterior chamber until the tip is centered on the optical axis (Figure 3D). With a sweeping motion, move the tip of the needle through the pupil, around the lens, and into the vitreous (Figure 3E). While rare, if the lens is nicked, the surgery should be abandoned.

Advance the needle tip to puncture the retina. The lens magnifies the view of the needle (Figure 3F). Once you encounter a slight resistance to the needle, STOP! You have reached the RPE layer. A gentle amount of pressure (the touch of which must be learned by experience) is applied to penetrate the neural retina into the subretinal space, but not so much that the tip penetrates or damages the RPE sheet. Being careful of the slightest of movement, use the foot pedal to inject fluid into the subretinal space. The nanojector system should be set to deliver 1000 nl at a rate of 170 nl/sec. It can be useful for an assistant to press the injection button on the face of the nanojector, but the footpedal is just as easy. Faster or slower injection rates have not been systematically investigated, but this rate provides acceptable filling of the subretinal space in our hands. Blood in the fundus means that the tip pressure was too great and the choroid was damaged. Too little pressure and the retina is not penetrated. Marker dye in the vitreous indicates the pressure was insufficient and the needle did not enter the subretinal space.

Leave the injection needle in the subretinal space for a few seconds to allow pressure in the injection system to equilibrate with subretinal bleb pressure, otherwise large fractions of the subretinal injection material will leak into the vitreous. Pull the needle out slightly, wait another second, and then remove needle entirely. Remove the needle slowly to allow the hole in the retina to reseal and to avoid damaging the lens, iris, and corneal endothelium during removal. After surgery, place more hydrogel on the cornea to examine the fundus.

A critical step is to count the number of large blebs (Figure 3H) on the fundus. Complete the post-op exam to confirm the presence of the blebs.

Place Triple antibiotic ointment (Taro Pharmaceuticals, Inc., Hawthorne, NY), which contains bacitracin, neomycin sulfate, and polymyxin B, on the eye. Verify the ear tag.

Recovery: Cover the animal on a 37 °C heating pad until it is awake and actively moving. Transfer it to a clean cage by itself for 1 to 2 h. Apply more Refresh every 10 minutes to keep corneas from drying out. Afterwards, return the mouse to its home cage until analysis, usually several days after treatment.

7. Worksheet: A record of the subretinal injection procedure should be kept. Documentation should include ear tag number (ear tags from WPI), date of birth, sex, amount of anesthesia, bleb size (small, medium, or large), and, especially important, the number of blebs. Also record any complications including backflow through the retinotomy, hemorrhage, lens damage, corneal clouding, or the presence of air bubbles. A qualitative comment on the outcome of each injection is encouraged.

8. Electroporation: Immediately following subretinal injection, any plasmid-treated mouse eyes or control (vehicle only) eyes are electroporated. Make electrodes by wrapping 20 gauge platinum-iridium wire around a sharpened pencil tip, creating a 1.5 to 2 mm loop. Clip the loops to jumper leads and then to the BTX electroporator. Position one platinum loop (anode) directly underneath the retina bleb site on the scleral surface of the mouse globe, and the other loop (cathode) should be positioned diametrically opposite from the retinotomy. Space the electrodes 1.5 to 2 mm apart. Try to be as consistent as possible in this spacing, as it determines the potential difference per cm, one of the critical variables in consistent transfection efficiency.

Optimal conditions and minimum requirements ought to be investigated by varying the voltage, pulse length, number of pulses, and number of pulse trains. With our apparatus, an optimum was found with 80 V, 5 pulses, 5 ms pulse duration, 1 s interval between pulses, and two pulse trains. The range of conditions that we tested were: 0.1 ms to 100 ms for pulse length, 0 to 200 V for potential difference, 5 to 20 pulses, 0.125 and 1 s interval between pulses, and one or two pulse trains.

Typical negative controls include omitting plasmid (vehicle-only subretinal injection) or omitting electroporation in different mice. The contralateral eye served as an uninjected control in all mice.

9. After experimentation, mice are euthanized by CO₂ asphyxiation.

10. Outcome measures of safety: For RPE cell sheets, TUNEL staining as a marker of apoptosis is an effective tool to assess damage. Flatmounts are created (44). Essentially, the eyecup flatmount includes all the cornea and sclera, but the neural retina, iris, ciliary body, and lens were removed (11, 45). A puncture was made in the cornea with a microknife, and iridectomy scissors (WPI) were used to make four radial cuts, starting at the center of the cornea, and extending toward the optic nerve. The flattened eyecups were placed on

microscope slides in 100 μ l of dPBS. Primary and secondary antibody staining solutions were pipetted on and off with handheld pipettors, but otherwise did not differ from standard immunostaining procedures. They are mounted in Vectashield hardset, and ought to be examined as soon as the hardset has fully solidified. We normally allow the mountant to set overnight and image the slides the next day.

11. Outcome measures of efficacy: Fluorescence detection of reporter gene expression. The tdTomato reporter gene has an excitation optimum at 554 nm, and a emission maximum at 581 nm. Compared to other naturally fluorescent proteins, tdTomato has reduced photobleaching and provides excellent fluorescence (46). TdTomato was excited using 561 nm laser line and emissions were filtered using a 605/75 bandpass filter.

3. Notes

1. Quantum Dots have a tendency to aggregate, clogging a 35 gauge needle and tubing in the injector system. To prevent clogging, it has been suggested that they be mixed with serum albumin at 0.5 mg/ml (47).

2. Basic subretinal injection procedure and videos. A video of the surgical procedure is given on the website (Figure 5), and highlight the correct techniques from Johnson and coworkers (1).

3. Potential pitfalls: The costs (in time and effort) associated with optimizing this procedure can be significant. Table 1 presents some of the problems we encountered with the injection technique and solutions we found.

4. Signs of a successful procedure: Careful examination of the adult mouse fundus, after surgery, is a good way to evaluate the success or failure of the injection. A thorough look at the fundus is a critical step.

For nonpigmented mice, three blebs underlying the neural retina is a sign of proper inflation of the subretinal space in the adult mouse eye. These blebs are clearly visible, and they demonstrate that the injected material was well confined within the subretinal space. We have not observed any cases of more than three blebs in nonpigmented mice. Eyes with only one or two blebs were usually accompanied by evidence of a torn or damaged retina, as seen on funduscopic examination. Nonpigmented mice without three blebs were excluded from experimental test groups.

For pigmented mice, we found that there were four blebs (Figure 4). The difference may lie in the more intense light source used for pigmented mice, or it may be a fundamental characteristic of the pigmented strains usually C57BL/6J that we routinely use.

There are several causes of incorrect inflation of the subretinal space: 1) material is injected into the vitreous; 2) fluid rapidly leaks out of the subretinal space into the vitreous through a hole in the retina; 3) retina is hopelessly torn; 4) material is injected elsewhere (cf., suprachoroidally or subchoroidally); 5) the pump does not operate correctly; or 6) the needle is clogged. Evidence of blood in the vitreous or aqueous, and nicking of the lens are major indicators of problems, and mice with these complications should be immediately excluded from subsequent experiments and analysis. All signs can be readily observed during fundus examination.

5. Expected results for expression of tdTomato: About 30-40% of RPE cells should express the reporter gene, in this case the red fluorescence from TdTomato (Figure 6). The

polygonal pattern of RPE cells is observed in both transfected and nontransfected cells, and there is no characteristic bias in the transfection of cells of lesser or greater polygonality.

6. Tissue death under optimized conditions should be <1% of RPE cells. An internal positive control for cell death is apoptosis in the corneal endothelium.

7. Expected injection success rate: This technique is successful in our hands about 80% of the time. It requires a significant amount of time to learn. Depending on the amount of practice and prior surgical skills, we find it takes 50–100 surgeries to become proficient in the subretinal injection of the adult mouse eye. This is in contrast to the relative ease in the subretinal injection of neonatal rat pups (28). We found the outcome of the surgery could be rapidly determined postoperatively by examining the mouse fundus. The subretinal injection raised blebs, indicating that the retina was elevated from the RPE sheet, and the persistence of these blebs demonstrated the retinal hole had sealed. No bleb meant that the surgery had failed, and the mouse should not be used for further experimentation. Initially, we expected only one large bleb, because that is what has traditionally been observed in subretinal injections of neonatal rat pups. However, we found the best outcomes were when there were three blebs in nonpigmented mice and four blebs in pigmented mice, and when the perimeters of these blebs, as viewed by funduscopy, were demarcated by major blood vessels. It should be noted that bleb formation is also used as a sign for successful subretinal injection in human patients (8, 10, 14, 47).

8. Expected results from electroporation: After electroporation, tdTomato fluorescence should be found in a tight patch of RPE cells nearest to the positive electrode (anode) (Figure 6). No fluorescence was detected at the negative electrode (cathode), which is nearer to the cornea. Accurate placement of the anode circumscribing the bleb and highly concentrated plasmid are necessary to achieve delivery of the plasmid into RPE cells and expression of tdTomato. Under suboptimal conditions, tdTomato fluorescence was detected in the cornea, ciliary body, and iris. This result occurred with much longer pulse durations (25 to 50 ms). Voltages beyond about 100 V resulted in immediate evidence of burn damage and were not tested further. Pulse lengths were varied from 1 ms to 50 ms at different voltages. At 10 ms or longer, the area of the flatmount that showed evidence of transfection extended beyond the immediate location of the electrodes as far as the cornea.

Acknowledgments

This work was supported by the National Eye Institute (R01EY016470, R01EY014026, P30EY006360, R24EY017045, T32EY007092), an unrestricted grant to the Department of Ophthalmology at Emory University from Research to Prevent Blindness, Inc., the Foundation Fighting Blindness, Fight for Sight, and the Intramural Research Program of the National Eye Institute.

References

1. Johnson CJ, Berglin L, Chrenek MA, Redmond TM, Boatright JH, Nickerson JM. Technical brief: subretinal injection and electroporation into adult mouse eyes. *Mol Vis*. 2008; 14:2211–2226. [PubMed: 19057658]
2. Yasukawa T, Ogura Y, Sakurai E, Tabata Y, Kimura H. Intraocular sustained drug delivery using implantable polymeric devices. *Adv Drug Deliv Rev*. 2005; 57:2033–2046. [PubMed: 16263193]
3. Schorderet DF, Manzi V, Canola K, Bonny C, Arsenijevic Y, Munier FL, Maurer F. D-TAT transporter as an ocular peptide delivery system. *Clin Experiment Ophthalmol*. 2005; 33:628–635. [PubMed: 16402957]
4. Maia M, Kellner L, de Juan E Jr, Smith R, Farah ME, Margalit E, Lakhnani RR, Grebe L, Au Eong KG, Humayun MS. Effects of indocyanine green injection on the retinal surface and into the subretinal space in rabbits. *Retina*. 2004; 24:80–91. [PubMed: 15076948]

5. Shen WY, Rakoczy PE. Uptake dynamics and retinal tolerance of phosphorothioate oligonucleotide and its direct delivery into the site of choroidal neovascularization through subretinal administration in the rat. *Antisense Nucleic Acid Drug Dev.* 2001; 11:257–264. [PubMed: 11572602]
6. Kimura H, Spee C, Sakamoto T, Hinton DR, Ogura Y, Tabata Y, Ikada Y, Ryan SJ. Cellular response in subretinal neovascularization induced by bFGF-impregnated microspheres. *Invest Ophthalmol Vis Sci.* 1999; 40:524–528. [PubMed: 9950614]
7. Maguire AM, Simonelli F, Pierce EA, Pugh EN, Mingozzi F, Bennicelli J, Banfi S, Marshall KA, Testa F, Surace EM, Rossi S, Lyubarsky A, Arruda VR, Konkle B, Stone E, Sun J, Jacobs J, Dell'Osso L, Hertle R, Ma Jx, Redmond TM, Zhu X, Hauck B, Zelenia O, Shindler KS, Maguire MG, Wright JF, Volpe NJ, McDonnell JW, Auricchio A, High KA, Bennett J. Safety and efficacy of gene transfer for Leber's congenital amaurosis. *The New England journal of medicine.* 2008; 358:2240–2248. [PubMed: 18441370]
8. Bainbridge JW, Smith AJ, Barker SS, Robbie S, Henderson R, Balaggan K, Viswanathan A, Holder GE, Stockman A, Tyler N, Petersen-Jones S, Bhattacharya SS, Thrasher AJ, Fitzke FW, Carter BJ, Rubin GS, Moore AT, Ali RR. Effect of gene therapy on visual function in Leber's congenital amaurosis. *N Engl J Med.* 2008; 358:2231–2239. [PubMed: 18441371]
9. Hauswirth WW. The consortium project to treat RPE65 deficiency in humans. *Retina.* 2005; 25:S60. [PubMed: 16374340]
10. Cideciyan AV, Aleman TS, Boye SL, Schwartz SB, Kaushal S, Roman AJ, Pang JJ, Sumaroka A, Windsor EAM, Wilson JM, Flotte TR, Fishman GA, Heon E, Stone EM, Byrne BJ, Jacobson SG, Hauswirth WW. Human gene therapy for RPE65 isomerase deficiency activates the retinoid cycle of vision but with slow rod kinetics. *Proc Natl Acad Sci USA.* 2008; 105:15112–15117. [PubMed: 18809924]
11. Berglin LC, Schmack I, Holley G, Nie X, Yang H, Grossniklaus HE, Edelhauser HF. Human RPE ex vivo 'Flatmount Technique' for Comparative Morphometric and Tissue Culture Survival Analysis (Mouse) Using Alizarin Red Staining, Live/Dead Cell Analysis and Epifluorescent Microscopy. *Invest Ophthalmol Vis Sci.* 2005; 46:3064.
12. Lai, Yu, Brankov, Barnett, Zhou, Redmond, Narfstrom, Rakoczy. Recombinant adeno-associated virus type 2-mediated gene delivery into the Rpe65^{-/-} knockout mouse eye results in limited rescue. *Genet Vaccines Ther.* 2004; 2:3. [PubMed: 15109394]
13. Pang JJ, Chang B, Hawes NL, Hurd RE, Davisson MT, Li J, Noorwez SM, Malhotra R, McDowell JH, Kaushal S, Hauswirth WW, Nusinowitz S, Thompson DA, Heckenlively JR. Retinal degeneration 12 (rd12): a new, spontaneously arising mouse model for human Leber congenital amaurosis (LCA). *Mol Vis.* 2005; 11:152–162. [PubMed: 15765048]
14. Nusinowitz S, Ridder WH 3rd, Pang JJ, Chang B, Noorwez SM, Kaushal S, Hauswirth WW, Heckenlively JR. Cortical visual function in the rd12 mouse model of Leber Congenital Amaurosis (LCA) after gene replacement therapy to restore retinal function. *Vision Res.* 2006; 46:3926–3934. [PubMed: 16814838]
15. Batten ML, Imanishi Y, Tu DC, Doan T, Zhu L, Pang J, Glushakova L, Moise AR, Baehr W, Van Gelder RN, Hauswirth WW, Rieke F, Palczewski K. Pharmacological and rAAV gene therapy rescue of visual functions in a blind mouse model of Leber congenital amaurosis. *PLoS Med.* 2005; 2:e333. [PubMed: 16250670]
16. Bainbridge JW, Mistry A, Schlichtenbrede FC, Smith A, Broderick C, De Alwis M, Georgiadis A, Taylor PM, Squires M, Sethi C, Charteris D, Thrasher AJ, Sargan D, Ali RR. Stable rAAV-mediated transduction of rod and cone photoreceptors in the canine retina. *Gene Ther.* 2003; 10:1336–1344. [PubMed: 12883530]
17. Dinculescu A, Glushakova L, Min SH, Hauswirth WW. Adeno-associated virus-vectorized gene therapy for retinal disease. *Hum Gene Ther.* 2005; 16:649–663. [PubMed: 15960597]
18. Balaggan KS, Binley K, Esapa M, MacLaren RE, Iqbal S, Duran Y, Pearson RA, Kan O, Barker SE, Smith AJ, Bainbridge JW, Naylor S, Ali RR. EIAV vector-mediated delivery of endostatin or angiostatin inhibits angiogenesis and vascular hyperpermeability in experimental CNV. *Gene Ther.* 2006; 13:1153–1165. [PubMed: 16572190]
19. Bemelmans AP, Bonnel S, Houhou L, Dufour N, Nandrot E, Helmlinger D, Sarkis C, Abitbol M, Mallet J. Retinal cell type expression specificity of HIV-1-derived gene transfer vectors upon

- subretinal injection in the adult rat: influence of pseudotyping and promoter. *The journal of gene medicine*. 2005; 7:1367–1374. [PubMed: 15966018]
20. Doi K, Hargitai J, Kong J, Tsang SH, Wheatley M, Chang S, Goff S, Gouras P. Lentiviral transduction of green fluorescent protein in retinal epithelium: evidence of rejection. *Vision Res*. 2002; 42:551–558. [PubMed: 11853772]
 21. Bloquel C, Bourges JL, Touchard E, Berdugo M, BenEzra D, Behar-Cohen F. Non-viral ocular gene therapy: potential ocular therapeutic avenues. *Adv Drug Deliv Rev*. 2006; 58:1224–1242. [PubMed: 17095114]
 22. Kamei M, Tano Y. Tissue plasminogen activator-assisted vitrectomy: surgical drainage of submacular hemorrhage. *Dev Ophthalmol*. 2009; 44:82–88. [PubMed: 19494655]
 23. Sandhu SS, Manvikar S, Steel DHW. Displacement of submacular hemorrhage associated with age-related macular degeneration using vitrectomy and submacular tPA injection followed by intravitreal ranibizumab. *Clin Ophthalmol*. 2010; 4:637–642. [PubMed: 20668667]
 24. Price J, Turner D, Cepko C. Lineage analysis in the vertebrate nervous system by retrovirus-mediated gene transfer. *Proc Natl Acad Sci U S A*. 1987; 84:156–160. [PubMed: 3099292]
 25. Gekeler F, Kobuch K, Schwahn HN, Stett A, Shinoda K, Zrenner E. Subretinal electrical stimulation of the rabbit retina with acutely implanted electrode arrays. *Graefes Arch Clin Exp Ophthalmol*. 2004; 42:587–596. [PubMed: 15197555]
 26. Pfeffer B, Wiggert B, Lee L, Zonnenberg B, Newsome D, Chader G. The presence of a soluble interphotoreceptor retinol-binding protein (IRBP) in the retinal interphotoreceptor space. *J Cell Physiol*. 1983; 117:333–341. [PubMed: 6686234]
 27. Gerding H. A new approach towards a minimal invasive retina implant. *Journal of neural engineering*. 2007; 4:S30–37. [PubMed: 17325414]
 28. Timmers AM, Zhang H, Squitieri A, Gonzalez-Pola C. Subretinal injections in rodent eyes: effects on electrophysiology and histology of rat retina. *Mol Vis*. 2001; 7:131–137. [PubMed: 11435999]
 29. Pachnis V, Pevny L, Rothstein R, Costantini F. Transfer of a yeast artificial chromosome carrying human DNA from *Saccharomyces cerevisiae* into mammalian cells. *Proc Natl Acad Sci USA*. 1990; 87:5109–5113. [PubMed: 2195548]
 30. Reeves, RH.; Cabin, DE.; Lamb, B. Introduction of large insert DNA into mammalian cells and embryos. In: Haines, Jonathan L., et al., editors. *Current protocols in human genetics/editorial board*. Vol. Chapter 5. 2001. Unit 5.12
 31. Tsong TY. Electroporation of cell membranes. *Biophys J*. 1991; 60:297–306. [PubMed: 1912274]
 32. Neumann E, Schaefer-Ridder M, Wang Y, Hofschneider PH. Gene transfer into mouse lymphoma cells by electroporation in high electric fields. *EMBO J*. 1982; 1:841–845. [PubMed: 6329708]
 33. Wong TK, Neumann E. Electric field mediated gene transfer. *Biochem Biophys Res Commun*. 1982; 107:584–587. [PubMed: 7126230]
 34. Taniyama Y, Tachibana K, Hiraoka K, Namba T, Yamasaki K, Hashiya N, Aoki M, Ogihara T, Yasufumi K, Morishita R. Local delivery of plasmid DNA into rat carotid artery using ultrasound. *Circulation*. 2002; 105:1233–1239. [PubMed: 11889019]
 35. O'Brien JA, Holt M, Whiteside G, Lummis SC, Hastings MH. Modifications to the hand-held Gene Gun: improvements for in vitro biolistic transfection of organotypic neuronal tissue. *Journal of neuroscience methods*. 2001; 112:57–64. [PubMed: 11640958]
 36. Felgner PL, Gadek TR, Holm M, Roman R, Chan HW, Wenz M, Northrop JP, Ringold GM, Danielsen M. Lipofection: a highly efficient, lipid-mediated DNA-transfection procedure. *Proc Natl Acad Sci USA*. 1987; 84:7413–7417. [PubMed: 2823261]
 37. Langer R. New methods of drug delivery. *Science*. 1990; 249:1527–1533. [PubMed: 2218494]
 38. Boussif O, Lezoualc'h F, Zanta MA, Mergny MD, Scherman D, Demeneix B, Behr JP. A versatile vector for gene and oligonucleotide transfer into cells in culture and in vivo: polyethylenimine. *Proc Natl Acad Sci USA*. 1995; 92:7297–7301. [PubMed: 7638184]
 39. Luo D, Saltzman WM. Synthetic DNA delivery systems. *Nat Biotechnol*. 2000; 18:33–37. [PubMed: 10625387]
 40. Gorman CM, Moffat LF, Howard BH. Recombinant genomes which express chloramphenicol acetyltransferase in mammalian cells. *Mol Cell Biol*. 1982; 2:1044–1051. [PubMed: 6960240]

41. Zheng QA, Chang DC. High-efficiency gene transfection by in situ electroporation of cultured cells. *Biochim Biophys Acta*. 1991; 1088:104–110. [PubMed: 1989690]
42. Li S, Tseng WC, Stolz DB, Wu SP, Watkins SC, Huang L. Dynamic changes in the characteristics of cationic lipidic vectors after exposure to mouse serum: implications for intravenous lipofection. *Gene Ther*. 1999; 6:585–594. [PubMed: 10476218]
43. Bins AD, van Rheenen J, Jalink K, Halstead JR, Divecha N, Spencer DM, Haanen JB, Schumacher TN. Intravital imaging of fluorescent markers and FRET probes by DNA tattooing. *BMC Biotechnol*. 2007; 7:2. [PubMed: 17201912]
44. Bodenstern L, Sidman RL. Growth and development of the mouse retinal pigment epithelium. I. Cell and tissue morphometrics and topography of mitotic activity. *Dev Biol*. 1987; 121:192–204. [PubMed: 3569658]
45. Berglin L, Mandell K, Schmack I, Holley G, Grossniklaus H, Parkos C, Edelhauser H. Reduction of Retinal Pigment Epithelium (RPE) Background Autofluorescence with Sudan Black Enhances Visualization of Fluorescently-Labeled Proteins in ex vivo RPE Flatmounts. ARVO Meeting Abstract. 2006:-----.
46. Shaner NC, Campbell RE, Steinbach PA, Giepmans BN, Palmer AE, Tsien RY. Improved monomeric red, orange and yellow fluorescent proteins derived from *Discosoma* sp. red fluorescent protein. *Nat Biotechnol*. 2004; 22:1567–1572. [PubMed: 15558047]
47. Hanaki K, Momo A, Oku T, Komoto A, Maenosono S, Yamaguchi Y, Yamamoto K. Semiconductor quantum dot/albumin complex is a long-life and highly photostable endosome marker. *Biochem Biophys Res Commun*. 2003; 302:496–501. [PubMed: 12615061]

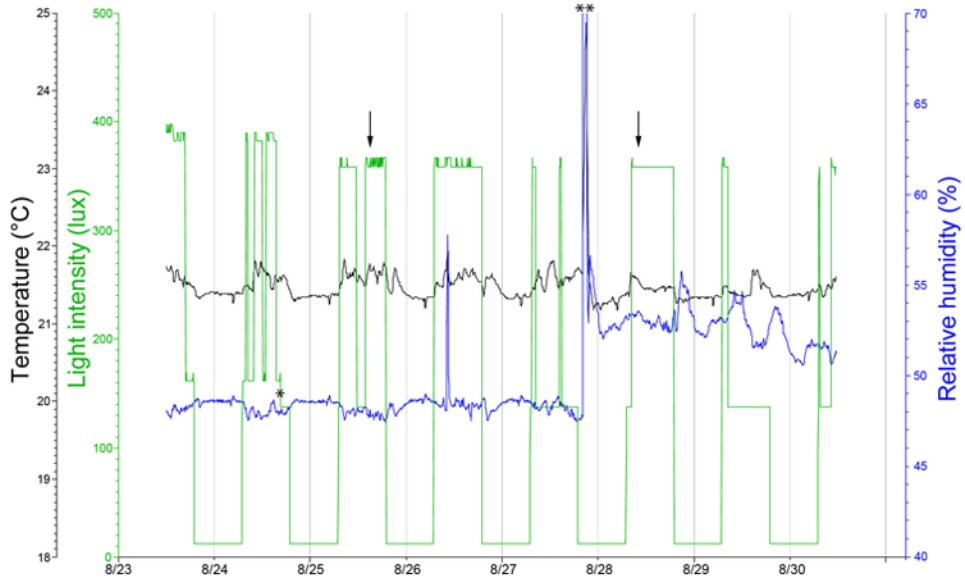


Figure 1. HOBOTraces. This set of traces represents a time period of one week in an animal room. A datalogger was positioned at the level of a middle row of cages. The green tracing represents light level. The blue tracing represents relative humidity, and the black tracing represents temperature. As an example of quirks that can go wrong in animal rooms that are difficult to detect, we found that a light switch was intermittently stuck in the high position, used when technicians work in this room. The switch should return the room to a light level of about 160 lux when the workers exit the room. With the switch in the high position, the middle row of cages receives about 380 lux. In this circumstance, cages at the top level, the light level is about 800 lux. This level on a 12 h on: 12 h off cycle is sufficient for mice to become preconditioned to high light levels. The light switch stuck in the “high” position are illustrated by arrows. A single asterisk represents a fluorescent light bulb burning out (shifting the normal lights on level from 160 lux to about 140 lux). A humidity spike (two stars) illustrates a substantial but short rain downpour outside the building. The temperature at about 21.5° C is quite consistent but the daytime temperature is generally higher than night by a fraction of a degree due to warming from fluorescent lights and normal building operations.

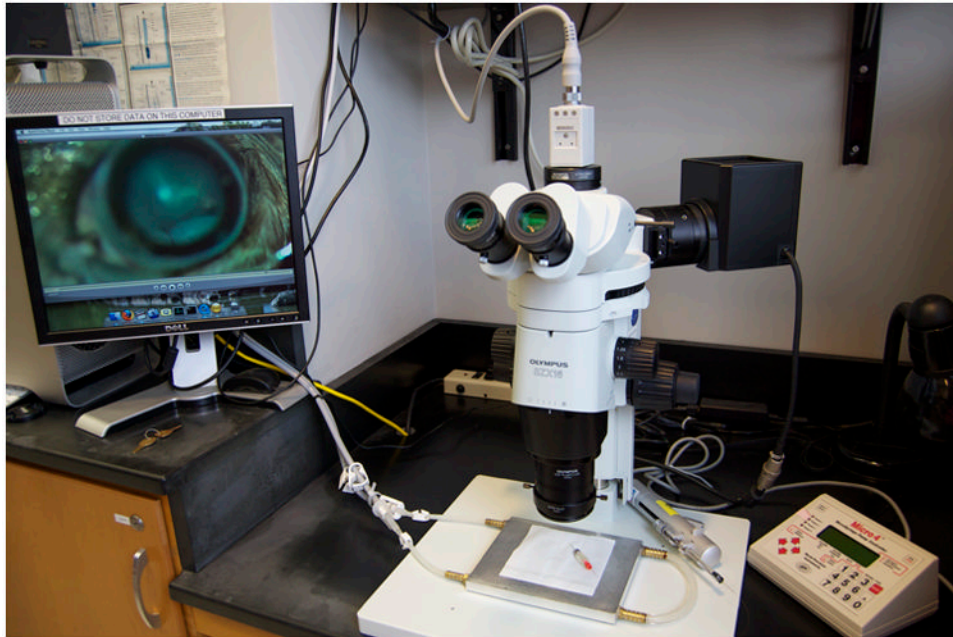


Figure 2. Injection and microscope setup. A conventional dissecting microscope is used with an epifluorescence halogen light source. A video camera is mounted to the microscope. A nanoliter injection system from WPI is employed. An air filter to the right suppresses dust and air currents at the injection station. A computer for control of the video camera and for video editing is partially pictured to the left. A homemade aluminum stage warmer is shown on the stage. Temperature is controlled with a Lauda circulating water bath. During surgery, the aluminum block is covered with a small rectangle of fresh spill paper.

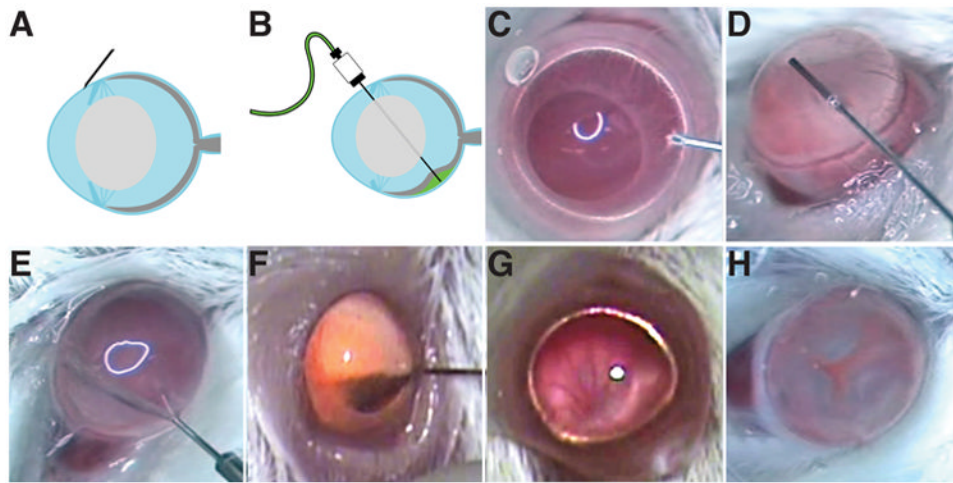


Figure 3.

The subretinal injection technique. A: Position of the 34 gauge beveled needle is shown nearly tangential just before lancing the cornea. B: Position of the 35 gauge blunt needle after puncturing the neural retina and partially inflating the interphotoreceptor space (the subretinal space) to produce subretinal blebs. Note that the needle is not running through the lens, but rather is running behind it. C: Presented is a still image from a video illustrating penetration of the cornea. D: This panel shows the positioning of the 35 gauge blunt needle in the center of the anterior chamber. E: The 35 gauge needle penetrates through the retina into the subretinal space. F: The 35 gauge needle is removed from the vitreous after subretinal injection of quantum dots. A small number of quantum dots are evident in the vitreous that generate a reddish-orange color. G: Illustrated is a fundus before subretinal injection. The retinal vessels can be readily detected in the fundus image. A ruddy red background color can be observed before injection. H: Shown is the fundus immediately after subretinal injection. The positions of three blebs surrounding the optic nerve head are located at clock face positions 4, 8, and 11. Each bleb appears puffy and gray in color with red vessels between the blebs. The optic nerve head is nearly centered in the image of the fundus. The imaged mouse eyes are about 3 mm in diameter. The caption and figure image are from Johnson et al (1). Reprinted with permission.

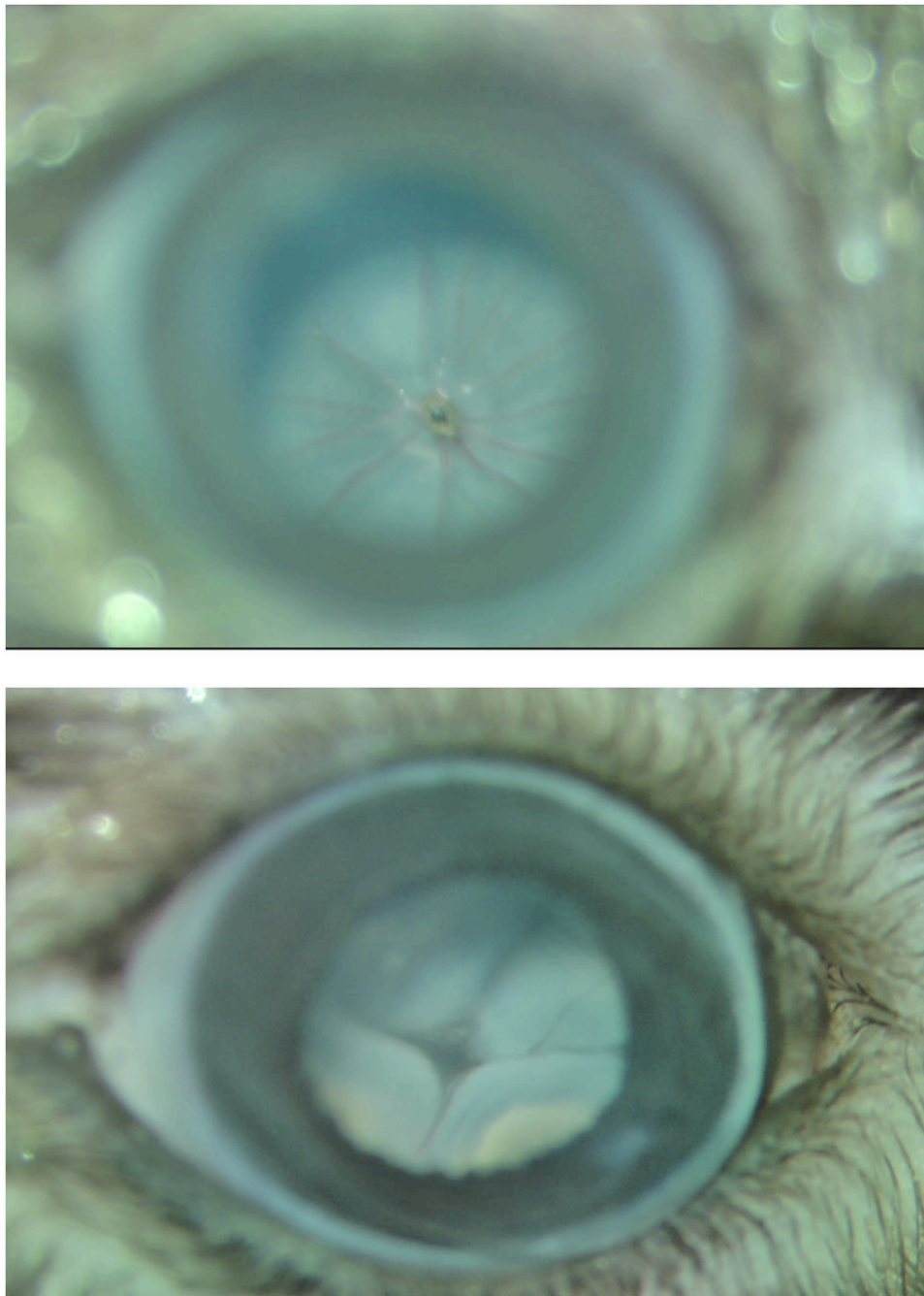


Figure 4. Four blebs in the fundus from a pigmented mouse eye after subretinal injection. Panel A. Fundus appearance before subretinal injection, and Panel B: After injection. Four blebs are readily apparent.



Figure 5. Video of subretinal injection by transcorneal route. This video was created on an Olympus dissecting microscope equipped with a ring light and an HD video camera. Double-click on the image to play the video. The orange color upon subretinal injection comes from the fluorescence of quantum dots, which demarcate the extent of the subretinal bleb. The slide bar at the bottom of the Quicktime movie can be used to manually control the flow of the movie. The caption and figure image are from Johnson and coworkers (1), reprinted with permission.

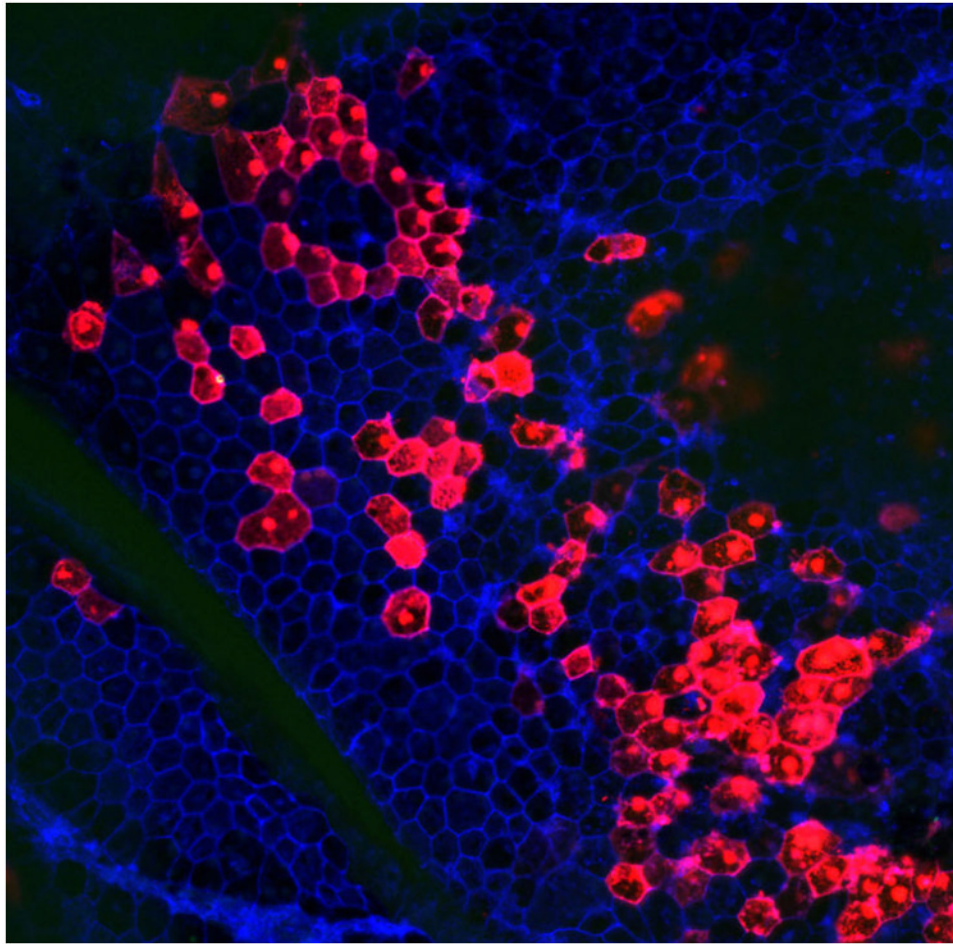


Figure 6. A typical result of subretinal injection and electroporation of the mouse eye. Transfection and expression of TdTomato were detected two days after injection. Red represents TdTomato protein fluorescence and blue represents actin rings stained with AlexaFluor688-phalloidin that mark the outline of the RPE cells. Both red hexagons and blue hexagons are readily detected in abundance near the injection site.

Table 1
Troubleshooting Guide for subretinal injections

Problem	Probable cause	Solutions
Lens cloudy	Lens capsule nicked during surgery	Avoid the lens.
No blebs	Not penetrating the retina	Press a little harder.
No blebs	Torn retina or retina hole; fluid leaks out quickly into vitreous	Penetrate retina in a single motion.
No blebs or a poorly inflated bleb	Fluid leaks out quickly into vitreous	Pause for 5–10 s before removing the blunt needle from the subretinal bleb. This allows pressure equilibration.
Blood	Penetrating into the choroid	Press gently.
Blood	Nicking the ciliary body	Sweep closer to lens.
Cloudy cornea	Eye was not kept moist before surgery	Apply lubricating eye drops between Proparacaine and phenylephrine application.
Air bubbles	Air in lines or solutions not degassed	Degas solutions. Flush the lines and prime them with water before filling with delivery solution.

From Johnson et al, with permission (1).